Emission color variation of $(Ba,Sr)_3BP_3O_{12}:Eu^{2+}$ phosphors for white light LEDs

Te-Wen Kuo,[1] Wei-Ren Liu[2] and Teng-Ming Chen[1]*

[1]*Phosphors Research Laboratory and Department of Applied Chemistry, National Chiao Tung University, Hsinchu 30010, Taiwan, R.O.C.*
[2]*Material and Chemical Research Laboratories, Industrial Technology Research Institute, Hsinchu 31014, Taiwan, R.O.C.*
tmchen@mail.nctu.edu.tw

Abstract: A series of alkaline earth borophosphate phosphors, $(Ba,Sr)_3BP_3O_{12}$ doped with Eu^{2+} ions, were synthesized by a solid state reaction. Two emission bands at 465 nm and 520 nm were attributed to the f–d transitions of doped Eu^{2+} ions occupying in two different cation sites in host lattices and emission color variation was observed by substituting the M^{2+} sites, which was rationalized in terms of two competing factors of the crystal field strength and bond covalence. Green and bluish-white pc-LEDs were fabricated by combination of a 370 nm near-UV chip and composition-optimized $Ba_3BP_3O_{12}:Eu^{2+}$ and $(Ba,Sr)_3BP_3O_{12}:Eu^{2+}$ phosphors, respectively. The series of phosphors may serve as a promising green and bluish-white luminescent materials used in fabrication of near UV-based white pc-LEDs.

OCIS codes: (250.5230) Photoluminescence; (160.2540) Fluorescent and luminescent materials.

References and links

1. Y. X. Pan, M. M. Wu, and Q. Su, "Tailored photoluminescence of YAG:Ce phosphor through various methods," J. Phys. Chem. Solids **65**(5), 845–850 (2004).
2. R. Mueller-Mach, and G. O. Mueller, "White-light-emitting diodes for illumination," Proc. SPIE **3938**, 30–41 (2000).
3. H. Wu, X. M. Zhang, C. F. Guo, J. Xu, M. M. Wu, and Q. Su, "Three-band white light from InGaN-based blue LED chip precoated with Green/red phosphors," IEEE Photon. Technol. Lett. **17**(6), 1160–1162 (2005).
4. K. Murakami, T. Taguchi, and M. Yoshino, "White illumination characteristics of ZnS-based phosphor materials excited by InGaN-based ultraviolet light-emitting diode," Proc. SPIE-Int. Soc. Opt. Eng. **4079,** 112–119 (2000).
5. Y. D. Huh, J. H. Shim, Y. H. Kim, and Y. R. Do, "Optical Properties of Three-Band White Light Emitting Diodes," J. Electrochem. Soc. **150**(2), H57–H60 (2003).
6. R. Kniep, H. Engelhardt, and C. Hauf, "A First Approach to Borophosphate Structural Chemistry," Chem. Mater. **10**(10), 2930–2934 (1998).
7. G. Blasse, A. Bril, and J. De Vries, "Luminescence of alkaline-earth borate-phosphates activated with divalent europium," J. Inorg. Nucl. Chem. **31**(2), 568–570 (1969).
8. A. Karthikeyani, and R. Jagannatan, "Eu^{2+} luminescence in *stillwellite*-type $SrBPO_{5-}$ a new potential X-ray storage phosphor," J. Lumin. **86**(1), 79–85 (2000).
9. Q. Su, H. B. Liang, T. Hu, Y. Tao, and T. Liu, "Preparation of divalent rare earth ions in air by aliovalent substitution and spectroscopic properties of Ln^{2+}," J. Alloy. Comp. **344**(1-2), 132–136 (2002).
10. P. Dorenbos, "Energy of the first $4f^7 \rightarrow 4f^6 5d$ transition of Eu^{2+} in inorganic compounds," J. Lumin. **104**(4), 239–260 (2003).
11. R. Kniep, G. Gözel, B. Eisenmann, C. Röhr, M. Asbrand, and M. Kizilyalli,, "Borophosphates–A Neglected Class of Compounds: Crystal Structures of $M^{II}[BPO_5]$(M^{II} = Ca, Sr) and $Ba_3[BP_3O_{12}]$," Angew. Chem. Int. Ed. Engl. **33**(7), 749–751 (1994).
12. Y. Shi, J. Liang, H. Zhang, Q. Liu, X. Chen, J. Yang, W. Zhuang, and G. Rao, "Crystal Structure and Thermal Decomposition Studies of Barium Borophosphate, $BaBPO_5$," J. Solid State Chem. **135**(1), 43–51 (1998).
13. Y. Shi, J. Liang, J. Yang, W. Zhuang, and G. Rao, "Subsolidus phase relations in the system $BaO-B_2O_3-P_2O_5$," J. Alloy. Comp. **261**(1-2), L1–L3 (1997).
14. G. Blasse, "Energy transfer in oxidic phosphors," Philips Res. Rep. **24**, 131 (1969).
15. L. G. Van Uitert, "Characterization of Energy Transfer Interactions between Rare Earth Ions," J. Electrochem. Soc. **114**(10), 1048–1053 (1967).
16. D. L. Dexter, "A Theory of Sensitized Luminescence in Solids," J. Chem. Phys. **21**(5), 836–850 (1953).

#119642 - $15.00 USD Received 6 Nov 2009; revised 26 Dec 2009; accepted 27 Dec 2009; published 15 Jan 2010

17. W. B. Im, Y. I. Kim, J. H. Kang, D. Y. Jeon, H. K. Jung, and K. Y. Jung, "Neutron Rietveld analysis for optimized $CaMgSi_2O_6:Eu^{2+}$ and its luminescent properties," J. Mater. Res. **20**(8), 2061–2066 (2005).
18. J. S. Kim, Y. H. Park, J. C. Choi, and H. L. Park, "Optical and Structural Properties of Eu^{2+}-doped $(Sr_{1-x}Ba_x)_2SiO_4$ phosphors," J. Electron. Soc. **152**(9), H135–H137 (2005).
19. N. K. Davidenko, and K. B. Yatsimirskii, Theoretical and Experimental Chemistry (New York: Springer), p505 (1973).
20. K. H. Bulter, Fluorescent Lamp Phosphors, The Pennsylvania State University Press, University Park, PA (1980).

1. Introduction

Nowadays, phosphor-converted light-emitting diodes (pc-LEDs) are potential candidates for solid-state lighting due to their excellent properties such as brightness, long lifetime, low applied voltage and high power efficiency [1–3]. Pc-LEDs can be easily fabricated by combining a blue or an ultraviolet (UV) LED chip with down-converting phosphors to generate white light. The first commercial pc-LED has been produced by the combination of blue LED with yellow-emitting cerium doped yttrium aluminum garnet (YAG:Ce) phosphor. However, this approach suffers from thermal quenching, poor color rendition and narrow visible range. Thus, much attention has been paid for the generation of white light, through a combination of red, green and blue phosphors with UV or near-UV (365–410 nm) LED. From the perspective of good color render index, seeking for highly efficient R/G/B-emitting phosphors under excitation wavelength in range of 350-410nm is important. Currently, the commonly used green-emitting phosphors for white LEDs are sulfide phosphors, such as ZnS:Cu, Al [4] and $SrGa_2S_4:Eu^{2+}$ [5], which show poor chemical stabilities against humidity and strong degradation upon LED chip pumping. Therefore, it is urgent to develop new green phosphors with comparatively modest synthesis and superior performance than sulfides.

In the last decade many borophosphates were reported and structurally characterized. The main structure features of borophosphates include planer BO_3 triangles or BO_4 tetrahedron sharing corners with PO_4 trtrahedra leading to a great variety of different structures with one-, two-, and three-dimensional anion complexes [6]. The divalent rare-earth Eu^{2+} ion has the $4f^7$ electronic configuration at the ground states and the $4f^65d^1$ electronic configuration at the excited states. The broadband absorption and luminescence of Eu^{2+} are due to $4f^7$–$4f^65d^1$ transitions. The emission of Eu^{2+}, strongly dependent on the type of host lattices, can vary from the ultraviolet to the red spectral range. The luminescence of Eu^{2+} ions in alkaline earth borophosphates with $M^{2+}BPO_5$ (M^{2+} = Ca, Sr, and Ba) composition have been studied by several groups [7–9] and these studies revealed that the Eu^{2+}-doped borophosphates could be photoluminescent materials with high efficiency. The absorption and emission bands of activators Eu^{2+} can also be well controlled by varying the crystal field or the bond covalence depending on site size, site symmetry and coordination environment of activator ions [10]. $Ba_3BP_3O_{12}$ was first prepared and structurally characterized by Kniep et al. [11]. The complex anion consists of linked tetrahedra only. In detail, central "vierer" single chains (BO_4 and PO_4 in alteration) run parallel to [001]; the two remaining oxygen vertices of each BO_4 tetrahedron are shared with a terminal PO_4 tetrahedron. $Ba_3BP_3O_{12}$ contains wide channels in which the barium ions are located. In this work, we report the luminescence of Eu^{2+}-doped $Ba_3BP_3O_{12}$, $Sr_3BP_3O_{12}$ and $(Ba,Sr)_3BP_3O_{12}$. The emission color variation attributed to the two emission bands of Eu^{2+} are also discussed from the perspective of crystal field strength and the covalence of hosts. Green and bluish-white pc-LEDs were also fabricated by combination of 370 nm LED chips and the as-synthesized phosphors.

2. Experimental

In this study, polycrystalline phosphors with compositions of $(Ba_{1-x-y}Sr_yEu_x)_3BP_3O_{12}$ were synthesized by a conventional solid state method. The raw materials were $BaCO_3$ (>99.9%, Aldrich), $SrCO_3$ (>99.9%, Aldrich), H_3BO_3 (99.9%, Aldrich), $NH_4H_2PO_4$ (>99%, Merck), and Eu_2O_3 (99.99%, Aldrich). Stoichiometric amounts of reactants were first well ground and intimately mixed in the requisite proportions; all powder samples were sintered at 950°C for 8

#119642 - $15.00 USD Received 6 Nov 2009; revised 26 Dec 2009; accepted 27 Dec 2009; published 15 Jan 2010

h in a reducing atmosphere of 15% H_2 and 85% N_2 in a furnace. The obtained products were pulverized for further characterizations.

The phase purity and crystal structure of as-prepared samples were characterized by powder X-ray diffraction (XRD) analysis with an advanced automatic diffractometer (Bruker AXS D8) with Cu Kα radiation (λ = 1.5418 Å) operated at 40 kv and 20 mA. The XRD data for phase identification were collected in 2θ range from 10 to 80°. The measurements of PL and PL excitation (PLE) spectra were performed by using a Spex Fluorolog-3 spectrofluorometer (Instruments S.A., Edison, N.J., USA) equipped with a 450 W Xe light source and double excitation monochromators. The powder samples were compacted and excited under 45° incidence, and emitted fluorescence was detected by a Hamamatsu Photonics R928 type photomultiplier perpendicular to the excitation beam. The spectral response of the measurement system was calibrated automatically on startup. To eliminate the second-order emission of the source radiation, a cutoff filter was used in the measurements. The CIE chromaticity coordinates for all samples were determined by a Laiko DT-100 color analyzer equipped with a charge coupled device (CCD) detector (Laiko Co., Tokyo, Japan). The electroluminescence (EL) spectra, color rendering index (CRI), and luminous efficiency of pc-LEDs were obtained at room temperature by using an integrating sphere (EVERFINE PHOTO-E-INFO Co. LTD).

3. Results and discussion

3.1 XRD profile analysis

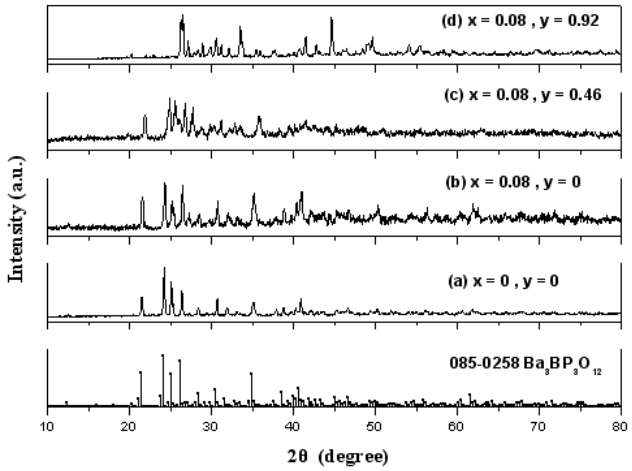

Fig. 1. XRD patterns of $(Ba_{1-x-y}Sr_yEu_x)_3BP_3O_{12}$ with (a) x = 0, y = 0; (b) x = 0.08, y = 0; (c) x = 0.08, y = 0.46; (d) x = 0.08, y = 0.92 and $Ba_3BP_3O_{12}$ (JCPDS file no. 085–0258).

The XRD patterns of the $Ba_3BP_3O_{12}$ and the composition-optimized phosphors of $(Ba_{0.92}Eu_{0.08})_3BP_3O_{12}$, $(Ba_{0.46}Sr_{0.46}Eu_{0.08})_3BP_3O_{12}$, and $(Sr_{0.92}Eu_{0.08})_3BP_3O_{12}$ are shown in Fig. 1. The diffraction peaks of $Ba_3BP_3O_{12}$, $(Ba_{0.92}Eu_{0.08})_3BP_3O_{12}$, and $(Ba_{0.46}Sr_{0.46}Eu_{0.08})_3BP_3O_{12}$ were found to be an orthorhombic structure and agree well with that reported by Shi et al. [12] and JCPDS card no. 085-0258. Among all $M_3BP_3O_{12}$ (M = Ca^{2+}, Sr^{2+}, and Ba^{2+}) phases, only $Ba_3BP_3O_{12}$ was obtained as a single phase, whereas other analogues of Ca^{2+} and Sr^{2+} were unknown phases or mixtures of known phases [12,13]. As shown in Fig. 2, Ba^{2+} ions have two different coordination numbers (CNs). Ba(1) and Ba(2) are eleven-coordinated ten-coordinated, respectively. According to the matching of ionic radii, the Eu^{2+} ions are expected to replace the Ba^{2+} ions in the host of $Ba_3BP_3O_{12}$.

#119642 - $15.00 USD Received 6 Nov 2009; revised 26 Dec 2009; accepted 27 Dec 2009; published 15 Jan 2010

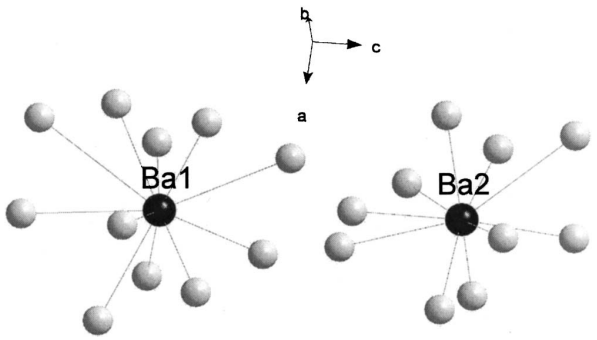

Fig. 2. Schematic representation for coordination of two different Ba^{2+} sites in $Ba_3BP_3O_{12}$ (Ba atoms, black spheres; O atoms, grey spheres).

3.2 PLE and PL spectra of $M_3BP_3O_{12}:Eu^{2+}$ (M = Ba, Sr) phosphors

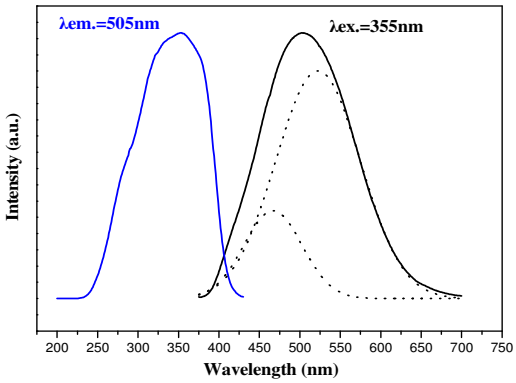

Fig. 3. PLE and PL spectra of $(Ba_{0.92}Eu_{0.08})_3BP_3O_{12}$ phosphor. ($\lambda_{ex.}$ = 355 nm, $\lambda_{em.}$ = 505 nm). The dotted lines are Gaussian decomposition curves

Figure 3 displays the PLE and PL spectra of $(Ba_{0.92}Eu_{0.08})_3BP_3O_{12}$ obtained at room temperature. The results show a broad emission band extending from 450 to 600 nm, which can be considered as a superposition of two Gaussian components with wavelengths peaking at 465 nm (P1) and 520 nm (P2), respectively. Two peaks merged at 505 nm where they were overlapped as a single band. The emission at 465 nm can be attributed to the Eu^{2+} ion occupying in the larger Ba(1) site with a weaker crystal field, whereas that peaking at 520 nm can be due to the Eu^{2+} ions in the smaller Ba(2) site with a stronger crystal field. The emission of $(Ba_{0.92}Eu_{0.08})_3BP_3O_{12}$ with intense and broad features were mainly originated from $5d\rightarrow4f$ transition of Eu^{2+} ions due to the strong coupling of the 5d electron with host lattice.

Figure 4 shows the PLE and PL spectra of $(Sr_{0.92}Eu_{0.08})_3BP_3O_{12}$ at room temperature. It exhibits a broad emission band extending from 400 to 450 nm, which could be considered as a superposition of two Gaussian components with wavelengths peaking at 400 nm (P1) and 440 nm (P2), respectively. The two peaks merged at 420 nm and they overlapped and merged as a single band. The PLE spectra of $(Ba_{0.92}Eu_{0.08})_3BP_3O_{12}$ and $(Sr_{0.92}Eu_{0.08})_3BP_3O_{12}$ show broad band ranging from 300 to 400 nm, attributed to the $4f^7\rightarrow4f^65d^1$ transition of Eu^{2+} ions. The broad excitation band well matches with the emission spectral range of NUV LED (350–400 nm).

#119642 - $15.00 USD Received 6 Nov 2009; revised 26 Dec 2009; accepted 27 Dec 2009; published 15 Jan 2010

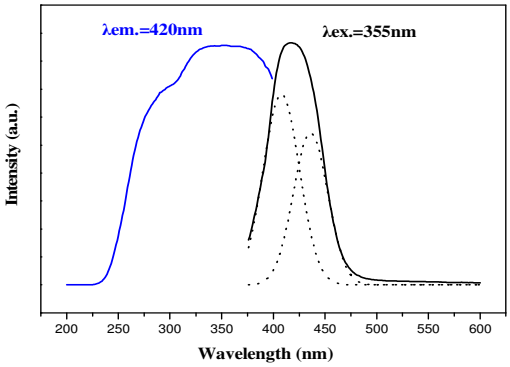

Fig. 4. PLE and PL spectra of $(Sr_{0.92}Eu_{0.08})_3BP_3O_{12}$ phosphor. ($\lambda_{ex.}$ = 355 nm, $\lambda_{em.}$ = 420 nm). The dotted lines are Gaussian decomposition curves.

3.3 Effect of Eu^{2+} concentration on luminescent properties of $(Ba_{1-x}Eu_x)_3BP_3O_{12}$

Figure 5 shows the PL spectra as a function of the Eu^{2+} concentration (x) for the $Ba_3BP_3O_{12}$:$x$$Eu^{2+}$phosphors. The data indicated that $(Ba_{0.92}Eu_{0.08})_3BP_3O_{12}$ is the optimized-composition. When considering the mechanism of energy transfer in oxide phosphors, Blasse [14] pointed out that if the activator is introduced solely on Z ion sites, x_c is the critical concentration, N the number of Z ions in the unit cell and V is the volume of the unit cell, then there is on the average one activator ion per V/x_cN. The critical transfer distance (R_c) is approximately equal to twice the radius of a sphere with this volume:

$$R_c \approx 2(\frac{3V}{4\pi x_c N})^{1/3} \quad (1)$$

Taking the values of V (2255 $Å^3$), N (16), and x_c (0.08), the R_c was calculated to be 15 Å. It was believed that the decrease in the PL intensity for samples with x of 0.08 was mainly due to the non-radiative transition among the Eu^{2+} ions, which may occur because of exchange interaction, radiation reabsorption, or multipole–multipole interaction [15,16]. The exchange interaction is generally responsible for the energy transfer of forbidden transitions and the typical distance is about 5 Å [15]. Because the 5d–4f transition of Eu^{2+} ion is allowed and the PLE and PL spectra were not well overlapped [Fig. 3 (a) and 3(b)], the non-radiative transitions among the Eu^{2+} ions took place via electric multipolar interactions according to Dexter theory [16,17]. The emission intensity (I) per activator concentration (x) can be expressed by the following equation [15,16]:

$$\frac{I}{x} = \frac{k}{1+\beta(x)^{\theta/3}} \quad (2)$$

where k and β are constants for each interaction for a given host lattice; θ = 6, 8, 10 for dipole–dipole, dipole–quadrupole, quadrupole–quadrupole interactions, respectively. Figure 6 illustrates the I/x dependence upon x on a logarithmic scale. The dependence of $\log(I/x)$ on $\log(x)$ was found to be relatively linear and the slope ($-\theta/3$) was determined to be −1.92. Thus, the value of θ could be calculated as 5.76, which was close to 6. This indicated that dipole–dipole interaction dominated the concentration quenching mechanism of Eu^{2+} emission.

#119642 - $15.00 USD Received 6 Nov 2009; revised 26 Dec 2009; accepted 27 Dec 2009; published 15 Jan 2010

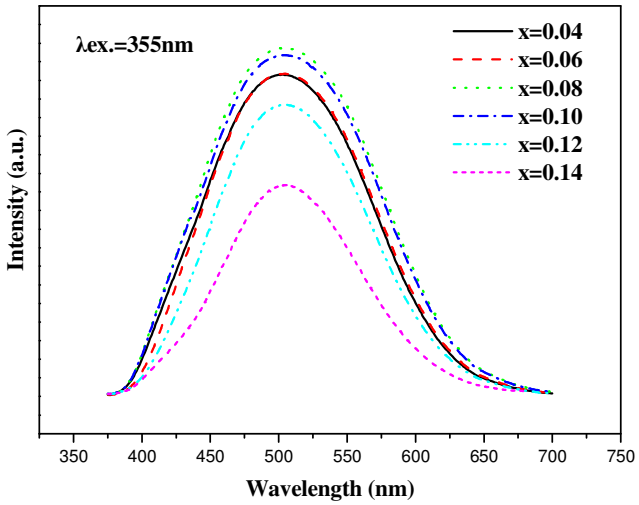

Fig. 5. Comparison of PL spectra for $(Ba_{1-x}Eu_x)_3BP_3O_{12}$ phosphors.

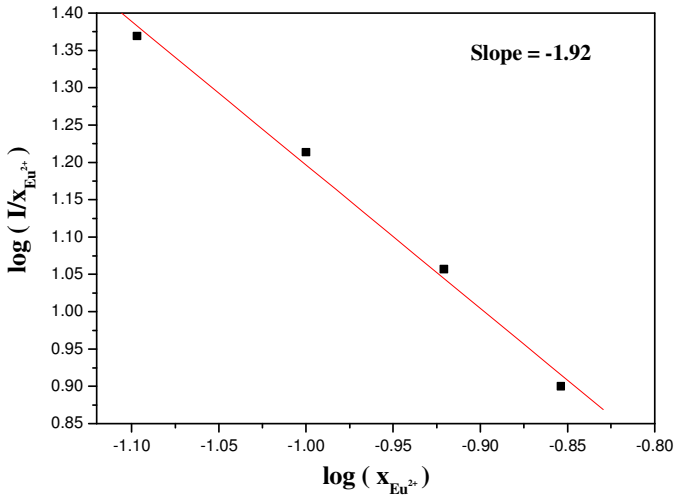

Fig. 6. The $\log(I/x_{Eu2+})$ dependence of $\log(x_{Eu2+})$ on a logarithmic scale.

3.4 Effect of Sr^{2+} concentration on photoluminescence of $(Ba_{0.92-y}Sr_yEu_{0.08})_3BP_3O_{12}$

Figure 7 shows the PL spectra of $(Ba_{0.92-y}Sr_yEu_{0.08})_3BP_3O_{12}$ (y = 0, 0.092, 0.276, 0.46, and 0.92). With substitution of Ba^{2+} for Sr^{2+} (i.e., from $Ba_3BP_3O_{12}$:Eu^{2+} to $Sr_3BP_3O_{12}$:Eu^{2+}), the emission bands of longer wavelength show blue-shifting, whereas these of shorter wavelength show red-shifting. This observation could be explained in terms of two competing factors: the crystal field and the bond covalence [10].

#119642 - $15.00 USD Received 6 Nov 2009; revised 26 Dec 2009; accepted 27 Dec 2009; published 15 Jan 2010

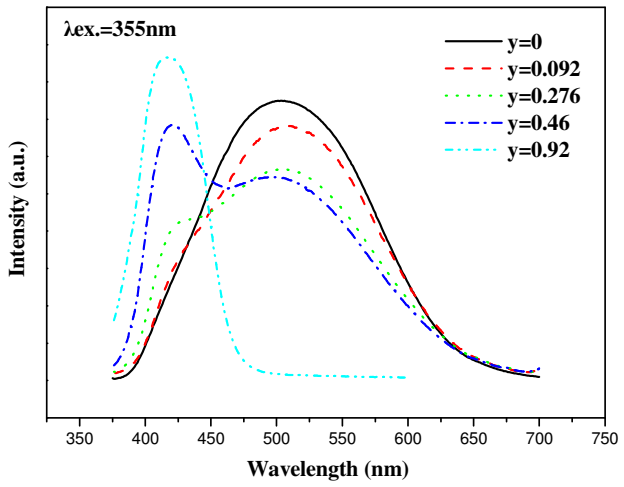

Fig. 7. Comparison of PL spectra of $(Ba_{0.92-y}Sr_yEu_{0.08})_3BP_3O_{12}$ phosphors.

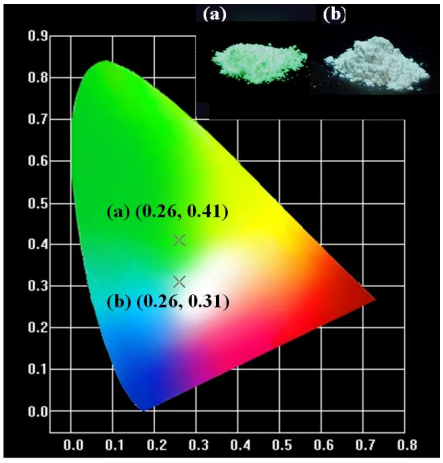

Fig. 8. CIE chromaticity diagram for (a) $(Ba_{0.92}Eu_{0.08})_3BP_3O_{12}$ and (b) $(Ba_{0.46}Sr_{0.46}Eu_{0.08})_3BP_3O_{12}$ excited at 355 nm. The inset shows the (a) $(Ba_{0.92}Eu_{0.08})_3BP_3O_{12}$ and (b) $(Ba_{0.46}Sr_{0.46}Eu_{0.08})_3BP_3O_{12}$ photos taken under 365 nm excitation in a UV box.

The crystal field strength increases with decreasing bond length by replacing Ba^{2+} with smaller Sr^{2+} cations. The correlation between the crystal field strength and bond length is given in the following equation [18],

$$D_q = 3Ze^2r^4/5R^5 \quad (3)$$

where D_q is the crystal field strength, R is the bond length between a center ion and ligands. Therefore, the increase in the crystal field could results in red shift for 5d→4f transition of Eu^{2+}, as indicated by Kim et al. [18] In addition, the observed blue shift could be explained in terms of the decreasing nephelanxetic effect [19]. With the decrease in the degree of covalence of Eu–O bonds in the order of Ba and Sr, less negative charge transfer to Eu^{2+} ions and thus increase the energy difference between the 4f and the 5d levels. Thus, the degree of covalence in the Eu–O bonds was decreased with substitution of Ba^{2+} with smaller Sr^{2+} cations and, consequently, the blue shifting of the Eu^{2+} emission band resulted.

#119642 - $15.00 USD Received 6 Nov 2009; revised 26 Dec 2009; accepted 27 Dec 2009; published 15 Jan 2010

In the case of $Ba_3BP_3O_{12}:Eu^{2+}$ to $Sr_3BP_3O_{12}:Eu^{2+}$, the size difference between the M(2) site and ionic radius of Eu^{2+} ion were too much larger than that between the size difference of M(1) site and that of Eu^{2+} ion. The symmetry of ligand ions surrounded Eu^{2+} ions was slightly distorted and their crystal fields were relaxed. Since ligand ions should not effectively exert the crystal field on Eu^{2+} ions occupying the M(2) sites. Consequently, the bond covalence effect in M(2) site was dominant and the covalence decreases in order of $Ba^{2+} > Sr^{2+}$ so that the slightly blue shift of $Eu^{2+}(2)$ emission at longer wavelength was observed. On the other hand, the difference between the size of M(1) site and ionic radius of Eu^{2+} ions was smaller than that between the size of M(2) site and that of Eu^{2+} ions. The Eu^{2+} ions occupying the larger M(1) site are dominantly affected by the crystal field causing the slightly red shift of $Eu^{2+}(1)$ emission at shorter wavelength.

Figure 8 shows the Commission International de I'Eclairage (CIE) chromaticity diagram with empirical CIE coordinates under excitation at 355 nm. The chromaticity coordinates of composition-optimized phosphors, $(Ba_{0.92}Eu_{0.08})_3BP_3O_{12}$ and $(Ba_{0.46}Sr_{0.46}Eu_{0.08})_3BP_3O_{12}$, were found to be (0.26, 0.41) and (0.26, 0.31), respectively. The inset shows photographs for green $(Ba_{0.92}Eu_{0.08})_3BP_3O_{12}$ and bluish-white $(Ba_{0.46}Sr_{0.46}Eu_{0.08})_3BP_3O_{12}$ phosphors under 365nm excitation.

3.5 Packaging of Pc-LED

In order to investigate the EL properties of our phosphors in near-UV-based LED, green and bluish-white pc-LEDs, with the surface mount device (SMD), were fabricated by combining $(Ba_{0.92}Eu_{0.08})_3BP_3O_{12}$ and $(Ba_{0.46}Sr_{0.46}Eu_{0.08})_3BP_3O_{12}$ with near-UV LED chips (370 nm), respectively. The phosphor blend was made by dispersing respective phosphor with 1:1 by wt % in a transparent silicone resin, and pc-LEDs were then fabricated by coating the LED chips with the epoxy resin. Their optical properties of the pc-LEDs were evaluated under a power of 1.1 watt at room temperature. Figure 9(a) is the EL spectrum of the as-fabricated green pc-LED. The emission band at 505 nm was clearly observed in the EL spectrum of the green pc-LED with the CIE coordinates of (0.26,0.40). As shown in Fig. 9(b), there are two bands at 420 nm and 505 nm in the EL spectrum of the bluish-white pc-LED with CIE coordinates of (0.25, 0.27). The luminous efficiency was found to be 5.2 lm/W for the green pc-LED and 5.1 lm/W for the bluish-white pc-LED, respectively.

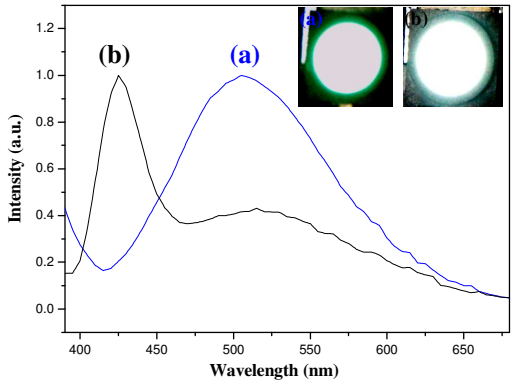

Fig. 9. EL spectra of (a) green LED fabricated with $(Ba_{0.92}Eu_{0.08})_3BP_3O_{12}$ and (b) bluish-white LED fabricated with $(Ba_{0.46}Sr_{0.46}Eu_{0.08})_3BP_3O_{12}$. The inset shows the green LED and bluish-white LED, both driven by a 350 mA current.

A qualitative criterion of the ability to display the colors of an irradiated object in a natural way is the color rendering index (CRI) [20]. The CIE coordinates, CRIs, and luminous efficiency of pc-LEDs are summarized in Table 1. Table 1 displayed the CRIs of the combination of near-UV LED with $(Ba_{0.46}Sr_{0.46}Eu_{0.08})_3BP_3O_{12}$, which gives a Ra of 81. The

#119642 - $15.00 USD Received 6 Nov 2009; revised 26 Dec 2009; accepted 27 Dec 2009; published 15 Jan 2010

CRI values based on the combination of near-UV LED with $(Ba_{0.46}Sr_{0.46}Eu_{0.08})_3BP_3O_{12}$ (Ra = 81) was found to be higher than that of commercial pc-LED (Harvatek Co. LTD, HT-P278BPV) that combining blue LED with YAG:Ce (Ra = 75).

Table 1. The comparison of commercial pc-LED and those were prepared by combining $(Ba_{0.92}Eu_{0.08})_3BP_3O_{12}$ and $(Ba_{0.46}Sr_{0.46}Eu_{0.08})_3BP_3O_{12}$ with NUV LED.

pc-LED	Power (watt)	CIE (x, y)	Ra	Luminous efficiency (lm/W)
Near-UV LED + $(Ba_{0.92}Eu_{0.08})_3BP_3O_{12}$	1.1	(0.26, 0.40)	56	5.2
Near-UV LED + $(Ba_{0.46}Sr_{0.46}Eu_{0.08})_3BP_3O_{12}$	1.1	(0.25, 0.27)	81	5.1
Blue LED + YAG:Ce (HT-P278BPV)	2.3	(0.32, 0.33)	75	28.1

For the application of high power LEDs, the thermal stability of phosphor is one of important issues to be considered. Temperature dependence of PL spectra for $(Ba_{0.92}Eu_{0.08})_3BP_3O_{12}$ under excitation at 355 nm is shown in Fig. 10. The inset displays and compares the thermal quenching property of $(Ba_{0.92}Eu_{0.08})_3BP_3O_{12}$ along with YAG:Ce^{3+} and Ba_2SiO_4:Eu^{2+} phosphors. As shown in Fig. 10, $(Ba_{0.92}Eu_{0.08})_3BP_3O_{12}$ exhibits good thermal stability as well as YAG:Ce^{3+} and is superior to that of silicate phosphor. The results indicate that for high power LED application, $(Ba_{0.92}Eu_{0.08})_3BP_3O_{12}$ could serve as a promising phosphor.

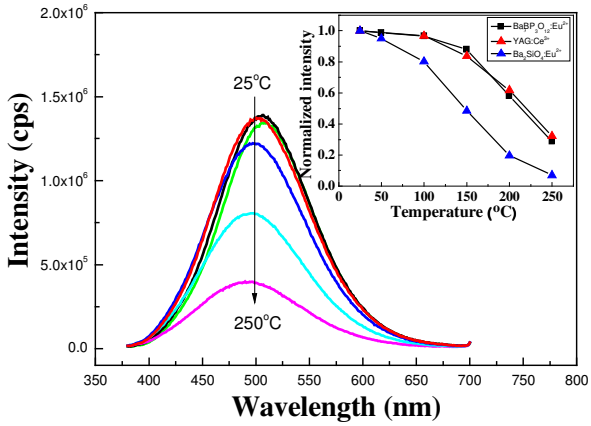

Fig. 10. Temperature dependent PL spectra for $(Ba_{0.92}Eu_{0.08})_3BP_3O_{12}$ excited at 355 nm. The inset shows the relationship PL intensity and temperature for $(Ba_{0.92}Eu_{0.08})_3BP_3O_{12}$. For comparison, commercial YAG:Ce^{3+} and Ba_2SiO_4:Eu^{2+} are also tested under their optimal excitation.

Figure 11 shows the decay curves for $(Ba_{1-x}Eu_x)_3BP_3O_{12}$ with various x and $(Sr_{0.92}Eu_{0.08})_3BP_3O_{12}$, respectively. We could successfully fit the decay curves based on the following multiple exponential equation,

$$I = A_1 \exp(\frac{-t}{\tau_1}) + A_2 \exp(\frac{-t}{\tau_2}) \quad (4)$$

where I represents the fluorescence intensity; A_1 and A_2 are constants; t is time; τ_1 and τ_2 are the decay times for the exponential components, respectively. By using fitting function, the parameters are calculated and summarized in Table 2. These results revealed that the decay curves of $Ba_3BP_3O_{12}$:xEu were independent of Eu^{2+} concentration. In addition, the decay curves could be well fitted by two-component exponential equation, indicating Eu^{2+} occupied

#119642 - $15.00 USD Received 6 Nov 2009; revised 26 Dec 2009; accepted 27 Dec 2009; published 15 Jan 2010

two different sites in $Ba_3BP_3O_{12}$ and $Sr_3BP_3O_{12}$ hosts. The results were consistent with PL data presented in Fig. 3 and 4. Table 2 summaries the corresponding parameters in these two phosphors, showing that τ_1 andτ_2 are ~100 μs and ~1200 μs for $Ba_3BP_3O_{12}:Eu^{2+}$ and ~186 μs and ~2872 μs for $Sr_3BP_3O_{12}:Eu^{2+}$, respectively.

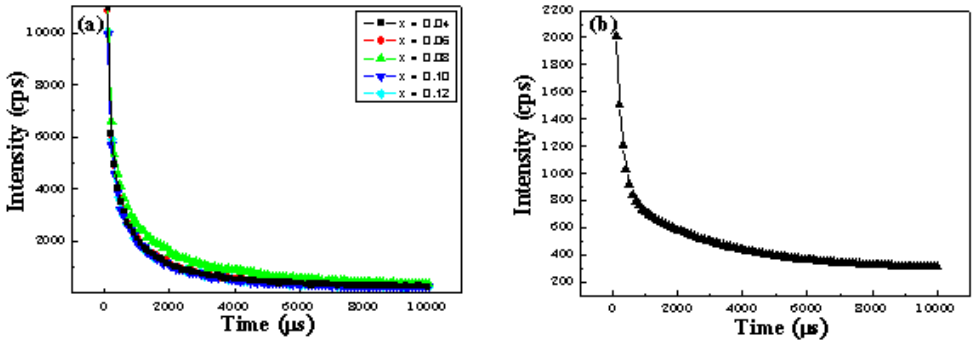

Fig. 11. The decay curves of as-synthesized phosphors excited at 355 nm and (a) monitored at 505 nm: $(Ba_{1-x}Eu_x)_3BP_3O_{12}$ and (b) monitored at 420 nm: $(Sr_{0.92}Eu_{0.08})_3BP_3O_{12}$.

Table 2. Comparison of decay times for $(Ba_{1-x}Eu_x)_3BP_3O_{12}$ and $(Sr_{0.92}Eu_{0.08})_3BP_3O_{12}$.

Compositions	Decay time (τ, μs) and constants (A)			
	A_1	τ_1	A_2	τ_2
$(Ba_{0.96}Eu_{0.04})_3BP_3O_{12}$	17,615	98.72	4,499	1,153.42
$(Ba_{0.94}Eu_{0.06})_3BP_3O_{12}$	17,876	95.88	4,523	1,150.12
$(Ba_{0.92}Eu_{0.08})_3BP_3O_{12}$	17,664	106.24	4,410	1,557.86
$(Ba_{0.90}Eu_{0.10})_3BP_3O_{12}$	14,794	107.77	4,025	1,237.36
$(Ba_{0.88}Eu_{0.12})_3BP_3O_{12}$	14,930	111.20	3,950	1,260.25
$(Sr_{0.92}Eu_{0.08})_3BP_3O_{12}$	1,978	186.25	588	2,872.15

4. Conclusion

In summary, a series of intense green and bluish-white emitting phosphors, $(Ba,Sr)_3BP_3O_{12}:Eu^{2+}$, were synthesized by a conventional solid state reaction. $(Ba_{0.92}Eu_{0.08})_3BP_3O_{12}$ and $(Sr_{0.92}Eu_{0.08})_3BP_3O_{12}$ showed emissions attributed to Eu^{2+} occupying in two sites with different coordination in the host lattices. Broad excitation band extending from 300 to 400 nm matches the emission spectral range of near-UV LEDs. Bright green and bluish-white LEDs were fabricated by the combination of 370 nm near-UV chips and the composition-optimized phosphors. The series of $(Ba,Sr)_3BP_3O_{12}:Eu^{2+}$ could serve as a promising green and bluish-white phosphor used in fabrication of near-UV excited LED. The high CRI values of the pc-LED demonstrate that $(Ba_{0.46}Sr_{0.46}Eu_{0.08})_3BP_3O_{12}$ phosphor may be suitable for application in solid-state lighting.

Acknowledgments

This research was supported by National Science Council of Taiwan, ROC under contract No. NSC98-2113-M-009-005-MY3 and by Industrial Technology Research Institute under contract no. 8301XS1751.

#119642 - $15.00 USD Received 6 Nov 2009; revised 26 Dec 2009; accepted 27 Dec 2009; published 15 Jan 2010